Modeling Surface and Subsurface Hydrologic Interactions in a South Florida Watershed near the Biscayne Bay

Hsin-Chi Jerry Lin[a*] Hwai-Ping (Pearce) Cheng[a], Earl V. Edris[a], and Gour-Tsyh (George) Yeh[b†]

[a]US Army Engineer Research and Development Center, Coastal and Hydraulics Laboratory, 3909 Halls Ferry Road, Vicksburg, MS 39180-6199

[b]University of Central Florida, Department of Civil and Environmental Engineering Orlando, FL 32816-2450

Restoration of the South Florida ecosystem is a major undertaking for the U.S. Army Corps of Engineers and the South Florida Water Management District. The Biscayne Bay Coastal Wetlands (BBCW) Project is one component of more than 60 restoration plans and has a goal to restore or enhance freshwater wetlands, tidal wetlands, and near shore bay habitat. The primary purpose of the BBCW project is to redistribute runoff from the watershed into the Biscayne Bay, away from the canal discharges that exist today and provide a more natural and historical overland flow through the existing and/or improved coastal wetlands. In an effort to restore wetlands, several structures, and management plans and scenarios are considered. One of the plans is to deliver fresh water from the existing canals through a shallow spreader swale system that is to distribute fresh water through wetlands into the Biscayne Bay. To achieve this, a tool is needed to design this complicated shallow spreader swale system. This paper presents how a spreader swale system, which includes 1D canal network routing, 2D overland flow, 3D subsurface flow, and flow through the interface of any two sub-domains of the spreader system, is simulated with the WASH123D computer code. A brief physics-based mathematical statements and numerical strategies of the model will be given. A hypothetical example that uses topographic data for the project area will be provided to demonstrate how WASH123D can help the design of a spreader swale system. Some issues that concerning the numerical convergence of the coupled flow model will also be discussed in this paper.

1. BACKGROUND

The Biscayne Bay Coastal Wetlands (BBCW) Project is one component of more than 60 restoration plans in the Comprehensive Everglades Restoration Plan (CERP) [1] and has a goal to restore or enhance freshwater wetlands, tidal wetlands, and near shore

*The work of this paper was supported by the U.S. Army Engineer District, Jacksonville (SAJ) and the South Florida Water Management District (SFWMD).

†Yeh was supported by the U.S. Environmental Protection Agency under grant No. R-82795602 with University of Central Florida.

bay habitat. The Biscayne Bay relies on substantial amounts of distributed freshwater to sustain its estuarine ecosystem. During the past century, field observations suggest that the delivery of freshwater to the Biscayne Bay has changed from overland sheet flow to one controlled by releases of surface water at the mouth of canals. The existing freshwater discharges to the bay are stressful to fish and benthic invertebrates in the bay near the canal outlets. Current restoration efforts in southern Florida are examining alternative water management plans that could change the quantity and the timing of freshwater delivery to the bay by restoring coastal wetlands along its western shoreline of the Biscayne Bay. One scenario to address this effort is to create a spreader swale system to redistribute available surface water entering the area from the regional canal system. The spreader swale system would consist of a delivery canal and shallow swales where water flows across the swale banks and becomes a more natural overland flow through existing coastal wetlands. Studying such scenario involves the modeling of a coupled flow system of 1D channel, 2D overland, and 3D subsurface.

2. THE WASH123D MODEL

The updated version of WASH123D [2] is used to study the spreader swale system. WASH123D is a physics-based [3], unstructured finite element model. The model is designed to simulate flow, chemical, and sediment transport in watershed systems. In modeling the flow of a coupled 1D channel, 2D overland, and 3D subsurface system, the following components are integrated in WASH123D, and the detail of these computations can be found in the WASH123D document [2].

2.1. Diffusion wave flow model using the semi-Lagrangian approach

The 1D diffusive wave flow equation can be stated as

$$\frac{\partial A}{\partial t} + \frac{\partial (AV)}{\partial x} = S_S + S_R - S_I + S_1 + S_2 \ , \tag{1}$$

where A is cross-sectional area at water depth h, V is cross-sectionally averaged velocity, S_S is man-induced source, S_R is rainfall, S_I is infiltration, S_1 and S_2 are contribution from overland flow through the channel banks. When the semi-Lagrangian method is used, (1) can be written as

$$\frac{dA}{dt} + A\frac{\partial V}{\partial x} = S_S + S_R - S_I + S_1 + S_2 \ . \tag{2}$$

Let $K = \frac{\partial V}{\partial x}$, (2) can discretized in time with the finite difference method as follows

$$\begin{aligned} \frac{{A_i}^{n+1} - {A_i}^{*}}{\Delta \tau} \quad = \quad & \frac{1}{2}\left[{(S_S + S_R - S_I + S_1 + S_2)_i}^{n+1} + {(S_S + S_R - S_I + S_1 + S_2)_i}^{*} \right] - \\ & \frac{1}{2}\left[{(KA)_i}^{n+1} + {(KA)_i}^{*} \right] \ . \end{aligned} \tag{3}$$

Here $\Delta \tau$ is the time interval of backward tracking, the combination of subscript "i" and superscript "$n+1$" is used to represent the variable/parameter at location x_i and the current time t^{n+1}, while the combination of subscript "i" and superscript "$*$" is used to represent the variable/parameter at location ${x_i}^*$ (i.e., the destination after backward tracking from x_i) and the time $t^{n+1} - \Delta\tau$. (3) can be further written as

$$\begin{aligned}\left(1 + \frac{\Delta\tau}{2}{K_i}^{n+1}\right){A_i}^{n+1} \quad = \quad & \left(1 - \frac{\Delta\tau}{2}{K_i}^{*}\right){A_i}^{*} + \frac{\Delta\tau}{2}\left[(S_S + S_R - S_I + S_1 + S_2)_i^{\ n+1} + \right. \\ & \left. (S_S + S_R - S_I + S_1 + S_2)_i^{\ *}\right] \ . \qquad (4)\end{aligned}$$

Let

$${D_i}^{n+1} = 1 + \frac{\Delta\tau}{2}{K_i}^{n+1} \ , \qquad {E_i}^{*} = 1 - \frac{\Delta\tau}{2}{K_i}^{*}$$

and

$$SS_i = \frac{\Delta\tau}{2}\left[(S_S + S_R - S_I + S_1 + S_2)_i^{\ n+1} + (S_S + S_R - S_I + S_1 + S_2)_i^{\ *}\right] \ ,$$

(4) can be simplified in form as

$${D_i}^{n+1}{A_i}^{n+1} = {E_i}^{*}{A_i}^{*} + SS_i \ . \qquad (5)$$

(5) can be solved node by node through the implementation of particle tracking. To ensure non-negative cross-sectional area, an adaptive explicit-implicit scheme can be used. Instead of solving (5), the following equation is solved when SS_i is found negative.

$$\left[{D_i}^{n+1} - \frac{SS_i}{{A_i}^{n+1,w}}\right]{A_i}^{n+1} = {E_i}^{*}{A_i}^{*} \ , \qquad (6)$$

where ${A_i}^{n+1,w}$ represents the updated value of ${A_i}^{n+1}$(or the value of the previous iterate).

To solve 2D diffusion wave flow model with the semi-Lagrangian approach, it is similar to solving 1D diffusion wave flow model as described above. When solving 3D Richards equations with the conventional finite element method, the numerical implementation can be found in the FEMWATER document [4].

2.2. Interactions between media

A rigorous coupling that does not introduce non-physics parameters holds the key to make a watershed model "truly" physics-based. The fluxes through the interfaces between media can be obtained without introducing any new parameter by imposing continuity of fluxes and state variables if all materials controlling the interactions are included [3].

2.2.1. Interactions between surface and subsurface waters

The fluxes between surface and subsurface media are obtained by imposing continuity of fluxes and state variables if these state variables do not exhibit discontinuity. If the state variables exhibit discontinuity, then a linkage term is used to simulate the fluxes. Consider the interaction between the 2D overland and 3D subsurface flows. When there is no impermeable layer on ground surface, it can be seen easily that the pressures in the overland flow (if present) and in the subsurface media will be continuous across the interface. Thus, the interaction must be simulated by imposing continuity of pressures and fluxes as

$$h^O = h^S \quad \text{and } Q^O = Q^S \quad \Longrightarrow \quad I = \mathbf{n}\cdot\mathbf{K}\cdot\left(\nabla h^S + \nabla z\right) \ , \qquad (7)$$

where h^O is the water depth in the overland if it is present, h^S is the pressure head in the subsurface, Q^O is the flux from the overland to the interface and Q^S is the flux from the interface to the subsurface media, I is the infiltration rate, $\mathbf{n}$ is an outward unit vector of the ground subsurface, and $\mathbf{K}$ is the hydraulic conductivity tensor. The use of a linkage term such as $Q^O = Q^S = K(h^O - h^S)$, while may be convenient, is not appropriate because it introduces a non-physics parameter K. The calibration of K to match simulations with field data renders the coupled model *ad hoc* even though the overland and subsurface flow models are each individually physics-based. The consideration of computing the flux through the 1D channel and 3D subsurface interface is the same as described above.

2.2.2. Interactions between channel and overland waters

Two cases are considered in the interaction of 1D channel and 2D overland waters. If the waters are connected, i.e., channel water stage is higher than the top of channel bank, the following continuity equations exist.

$$q^O = q^C \qquad \Longrightarrow \qquad S_1 = \mathbf{n} \cdot \mathbf{V}^O h^O \qquad \text{and} \qquad H^O = H^C \ , \tag{8}$$

where H^O is the water stage in the overland, H^C is the water stage in the channel, q^O is the outward normal flux of the overland flow, q^C is the lateral flow from overland to channel, S_1 is the normal flux from overland to channel, $\mathbf{n}$ is an outward unit vector (from the 2D overland side), $\mathbf{V}^O$ is overland flow velocity, and h^O is overland water depth. On the other hand, when the waters are separated, i.e., channel water stage is below the top of channel bank, water may flow from overland to channel only, and the following equations govern the interaction.

$$q^O = q^C = f(h^O) \qquad \Longrightarrow \qquad S_1 = \mathbf{n} \cdot \mathbf{V}^O h^O = f(h^O) \tag{9}$$

where f(h^O) is a prescribed function of h^O given by the shape and width of the channel bank. Since it is allowed in WASH123D that the two channel banks corresponding to a channel node may have different elevations, it is then possible that (8) is used for the interaction through one bank and (9) for the other. This feature is a MUST for studying the spreader swale system because it is likely in practice that the two banks of the spreader canal do not share the same elevation due to either design or topographical restriction.

2.2.3. Coupling 1D, 2D, and 3D flow

Figure 1 depicts the coupling structure employed in WASH123D. Ideally, channel, overland, and subsurface flows are strongly coupled within each time step. However, this would introduce unaffordable computation because small time step sizes are usually required for resolving 1D channel routing. To make computation affordable, in WASH123D each 3D flow time step may contain more than one 2D flow time steps and each 2D flow time step more than one 1D flow time steps. The fluxes through the surface-subsurface interface are updated using (7) for 2D/3D coupling and for 1D/3D coupling in each 3D coupling/nonlinear iteration, and in each 2D coupling/nonlinear iteration the fluxes through the channel-overland interface are computed using (8) and (9) for 1D/2D coupling.

3. A Hypothetic Example

This example demonstrates the capability of WASH123D in modeling a spreader swale system that includes 1D spreader canal, 2D overland, and 3D subsurface flow. It used the

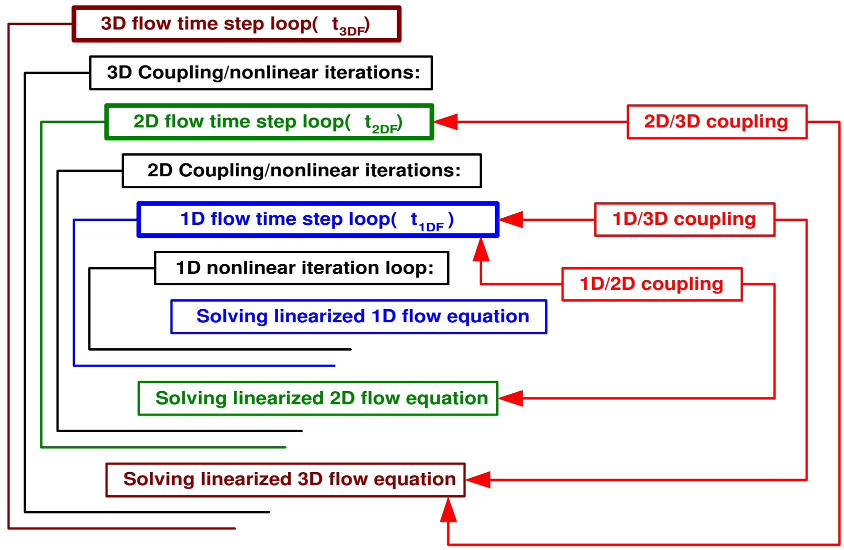

Figure 1. Coupling structure in WASH123D

topographic data in BBCW project area to construct the discretized domain of interest. A spreader canal was placed in the domain to distribute water that came in from the north boundary (marked with a red A in Figure 2). The 2D overland domain, which covered an area of approximately 26 square miles, was discretized with 10,784 triangular elements and 5,565 nodes. The 1D spreader canal embraced 136 elements, 139 nodes, one upstream boundary node, two dead ends, and one junction to connect the three canal reaches (Figure 2). The underlying 3D domain contained 53,920 elements and 33,390 nodes. Without the channel-related elements taken into account, the 2D computational domain actually contained 10,240 elements and 5,426 nodes. The width of the rectangular canal was 90 ft for Reach 1, 30 ft for Reach 2, and 50 ft for Reach 3 (Figure 2). The cross-sectional area was proportional to the depth, where the depth of the spreader canal was computed.

The Manning's roughness was set to 0.01 for 2D overland flow and 0.008 for 1D canal flow. The subsurface medium was sandy loam and was assumed isotropic, where the saturated hydraulic conductivity was 1,000 ft/day. The soil retention curves for the unsaturated zone were generated with the van Genuchten functions.

In computing 1D canal flow, a time-dependent water stage was given in Table 1 as the upstream boundary condition for the incoming water as indicated in Figure 2; a zero-velocity condition was applied at the two downstream dead-end nodes; and the continuity of both flow rate and water stage was enforced at the canal junction. In computing 2D overland flow, on the upstream stage boundary (Figure 3) a time-dependent water stage boundary condition was specified the same as that for 1D spreader canal (i.e., Table 1); a depth-dependent flux (i.e., rating curve) was given on the downstream depth-dependent (rating curve) boundary (Figure 3); and a channel-overland interaction boundary condition was specified for the channel-related overland boundary sides, which includes (1) a depth-dependent flux when water flowed from overland to canal and overland water and

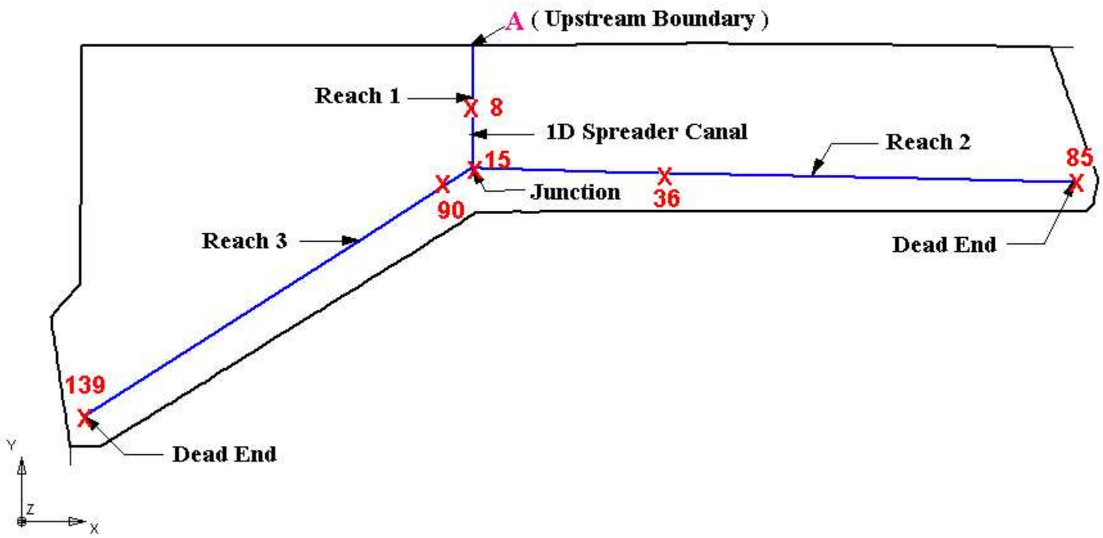

Figure 2. Features in the 1D spreader canal

canal water were separated and (2) a canal stage condition when flooding occurred (i.e., when overland water and canal water were connected). In computing 3D subsurface flow, an interface boundary condition that accounted for the interaction between surface and subsurface waters was applied to the top boundary face of the 3D domain; an impermeable boundary condition was assumed for the bottom boundary face; three total head boundary conditions were employed for three separate portions of the vertical boundary face as shown in Figure 4: a constant head of 3.5 ft for Portion A, a constant head of 1.2 ft for Portion B, and for Portion C a time-dependent head that was consistent with the 2D upstream water stage boundary condition; and an impermeable boundary condition for the rest of the vertical boundary face. It is noted that for the vertical boundary face with total head specified, the Dirichlet boundary condition applied only to the boundary nodes below water table (i.e., in the saturated zone). For the vertical boundary face that was above water table, an impermeable boundary condition was assumed.

Table 1
Time-dependent water stage given at the specified upstream canal/overland boundary nodes

Times(s)	0	600	3,600	7,200	129,600
Water State(ft)	2.25	2.25	2.50	2.98	2.98

The initial pressure head in the subsurface was computed by solving the steady-state version of Richards' equation with a constant rainfall rate of 2.3×10^{-9} ft/s, while a constant water depth of 0.46 ft was enforced at the 3D boundary nodes that were cor-

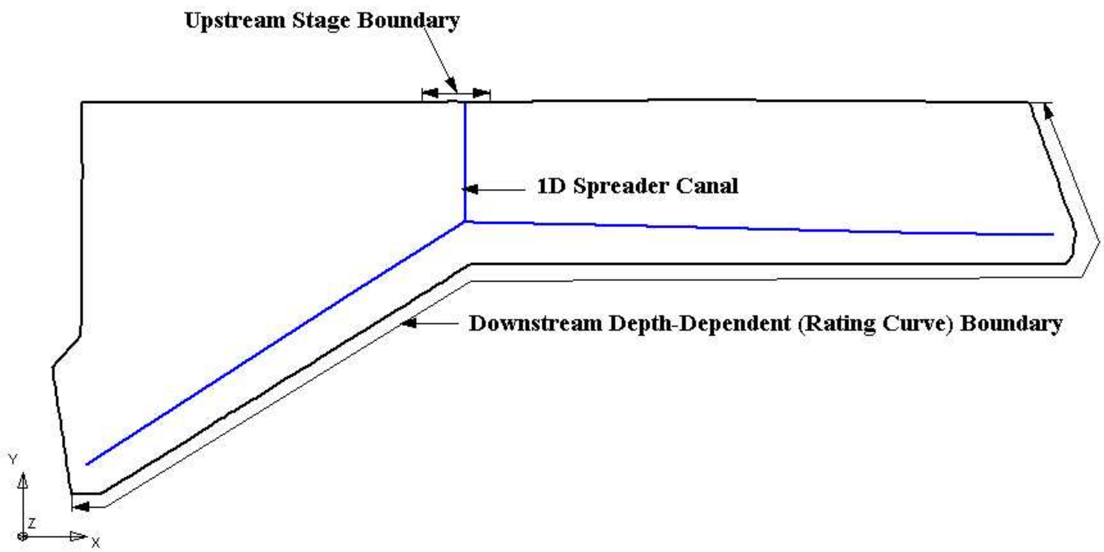

Figure 3. Specification of 2D overland boundary conditions

responding to 1D spreader canal nodes and zero water depth was assumed at those corresponding to 2D overland nodes. Such setup allowed us to expect water flow from the spreader canal to its neighboring overland regime within a short period of time after the transient simulation began. As the transient simulation started, a constant rainfall rate of 2.3×10^{-9} ft/s was applied throughout the entire simulation period of 36 hours. The time-step size was 240 seconds for computing 3D subsurface flow, from 1 to 10 seconds for computing 2D overland flow, and 0.1 second for computed 1D canal flow. The absolute error tolerance was 1.0×10^{-5} ft for determining nonlinear convergence in computing 1D, 2D, and 3D flow.

Figure 5 plots the variation of canal water depth at the 6 nodes indicated in Figure 2 from Time = 0 through 6 hours. It is observed from the numerical results that the changes of water stage at the six selected locations were negligible after Time = 18 hours (not shown here). Also, a dash line that represents the bank height over which canal water will merge with overland water is given in Figure 5 as reference for each node (marked with respective colors). The symbol of cross is used in Figure 5 to indicate the moments that water started to flow from canal to overland at respective nodes. Figure 6 shows the distribution of water depth on the 2D overland at various times (at 3, 6, 12, and 36 hours). It is seen that water from the spreader canal to overland only covered a limited portion of the entire 2D overland domain, which was due to the flat terrain considered herein. Close examination confirms that the numerical results of water depth of 1D canal and 2D overland are consistent with each other: flooding started to appear around 1D Nodes 8, 15, 90, and 139 before Time = 3 hours; flooding began at between Time = 3 hours and Time = 6 hours around Node 85; and no flooding ever happened around Node 36. Figure 7 shows the flow velocity vector near the junction at various times, where the overland water, after coming out of the spreader canal, moved by following the terrain downhill direction. Figure 8 plots the water table of subsurface flow at various times,

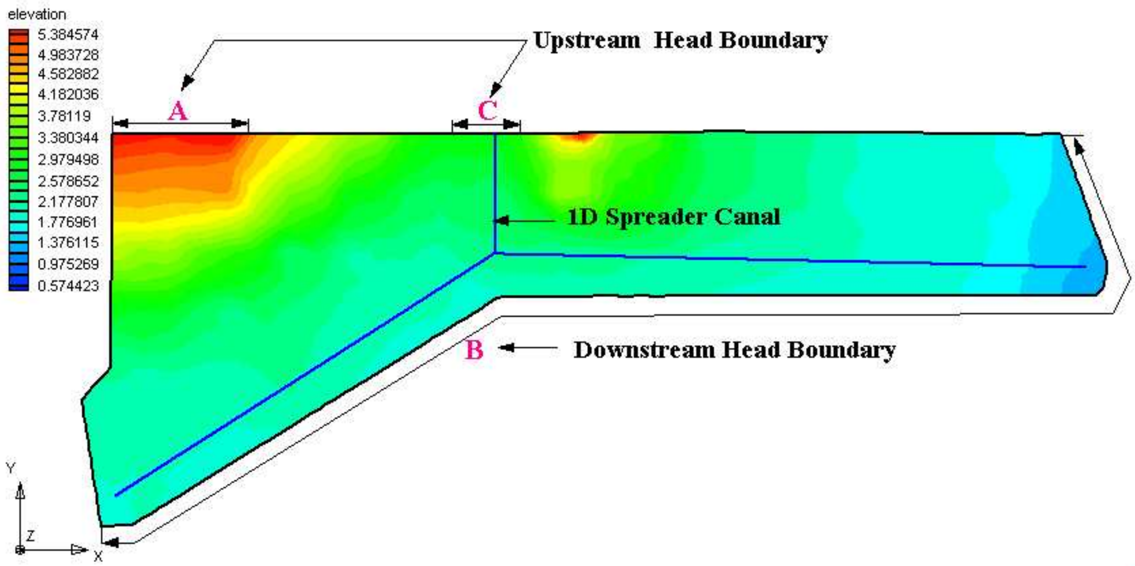

Figure 4. Specification of 3D subsurface boundary conditions

where water table was below ground surface for the area shaded with blue color and above ground surface for the no-shade area. It is obvious that Figures 6 and 8 match with each other very well. The consistency among Figures 5 (1D results), 6 (2D results), and 8 (3D results) verifies a correct implementation of coupled 1D/2D/3D flow in WASH123D.

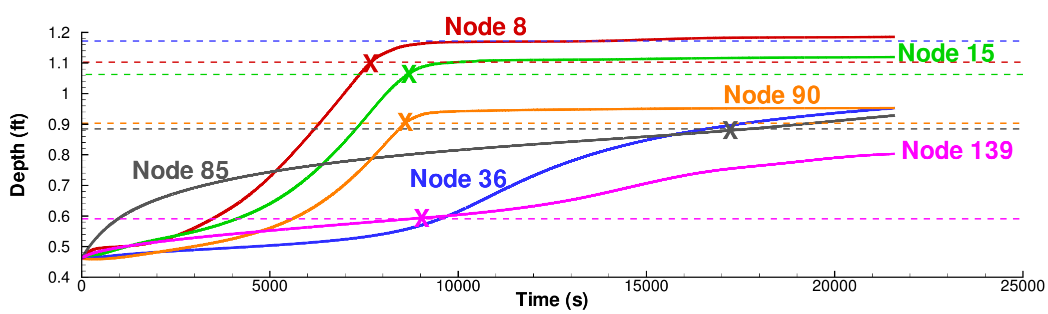

Figure 5. Computed water depth at various 1D canal locations (0 through 6 hours)

4. DISCUSSION

During the numerical simulation of the test example above, several numerical issues were revealed. Firstly, a very small time step is required due to the existence of dead ends in the system. When the canal flow toward a dead end along the downstream direction, the canal water is stopped (i.e., velocity equals zero) and piled up at the dead end. As a result, a backwater-like phenomenon may occur near the dead end, and the time step

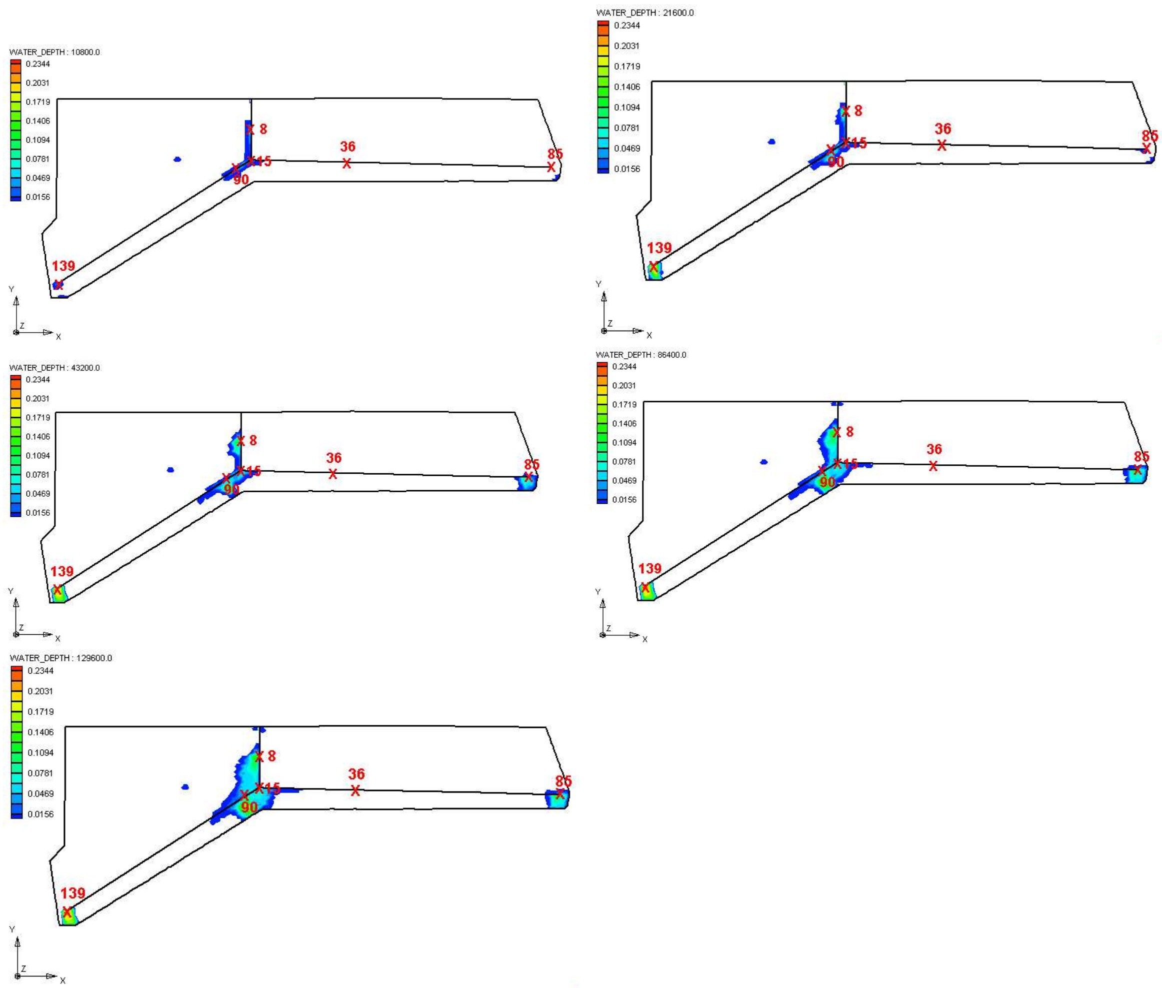

Figure 6. Distribution of overland water depth at various times: Time = 3 hours at Top Left, Time = 6 hours at Top Right, Time = 12 hours at Middle Left, Time = 24 hours at Middle Right, Time = 36 hours at Bottom

size must be small enough to stabilize the numerical outcome. Through some numerical experiments, it is observed that smaller canal elements require smaller time steps. It is also observed that after the canal water elevation exceed the bank top and flow over the bank to the neighboring overland at around the dead end, the constraint mentioned above can be relieved because the pile-up of water at the dead end vanishes. Secondly, the time step size of 3D flow is greatly affected by the surface-subsurface interaction. Large 3D time step sizes seem to help reduce computational effort because one large 3D time step may include many 2D time steps and even more 1D time steps. However, since the 3D pressure head and 1D/2D water depth are closed related to each other via the flux through the surface-subsurface interface, the use of large 3D time steps may cause convergence problem or produce inaccurate results. We have observed, from some numerical experiments, that strong coupling between surface and subsurface flow modules usually requires very small 3D time steps during the transition period when ground surface is from dry to wet, or

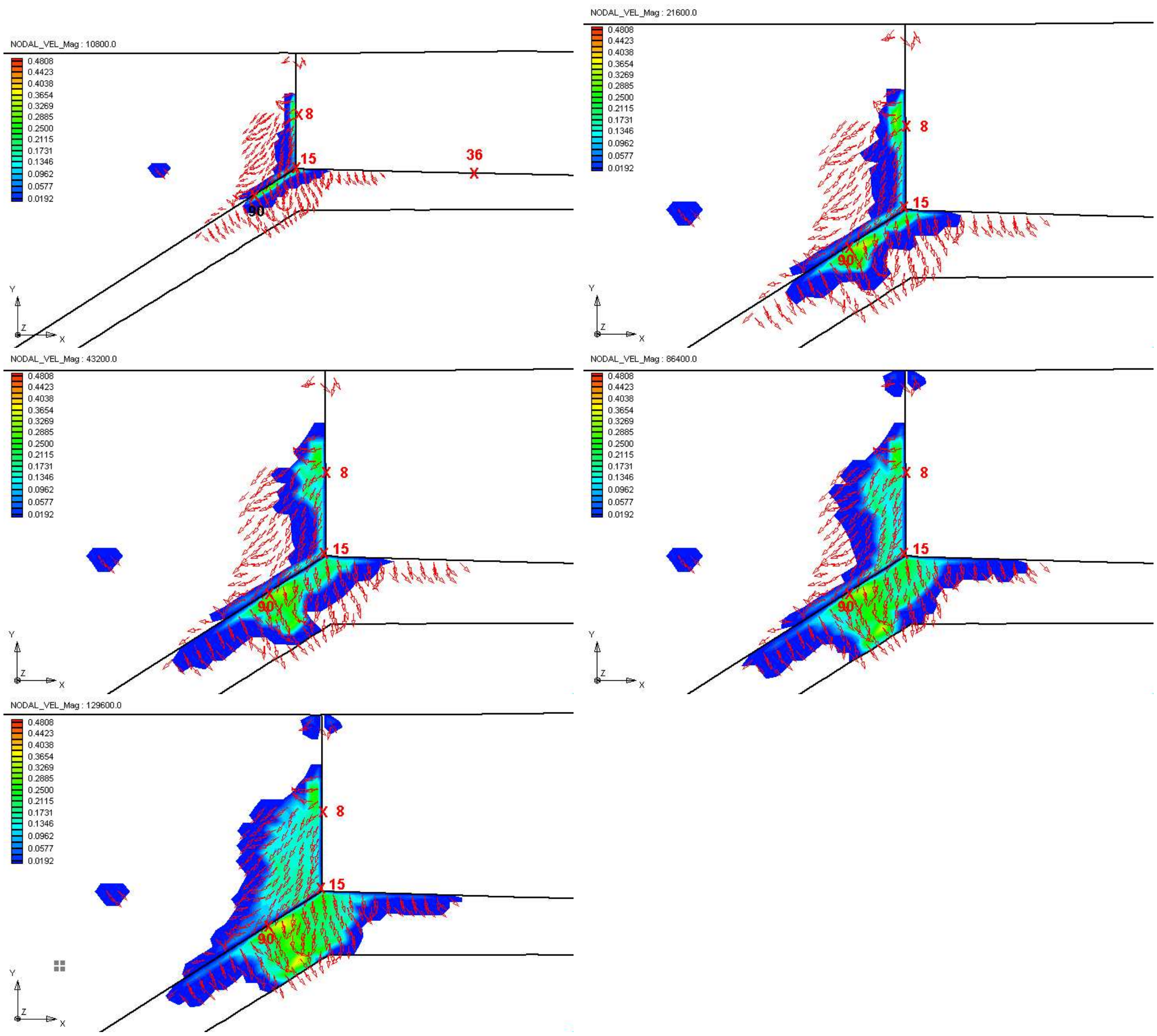

Figure 7. Velocity vectors of overland near the junction at various times: Time = 3 hours at Top Left, Time = 6 hours at Top Right, Time = 12 hours at Middle Left, Time = 24 hours at Middle Right, Time = 36 hours at Bottom

vice versa, which will make long-term simulations unachievable. To solve this problem, we propose that one uses 3D time steps smaller enough to resolve important physical phenomena and employs the weak coupling scheme (i.e., compute the interface flux based on the results at the previous 3D time) to account for surface-subsurface interactions.

Finally, there exists a dilemma in constructing computational grids for large-scale watersheds. Although the semi-Lagrangian approach allows us to more efficiently solve linearized 1D and 2D flow equations and guarantees non-negative water depth when the adaptive explicit-implicit scheme is also applied, it is noted that the time step size must be small enough for reaching nonlinear convergence. Since larger computational grids (i.e., Dx) will allow larger time steps, we should, without sacrificing important topographical information, make our 1D and 2D elements as large as possible so that we can use larger time steps and save computer time. However, if the 2D overland grid also aligns with

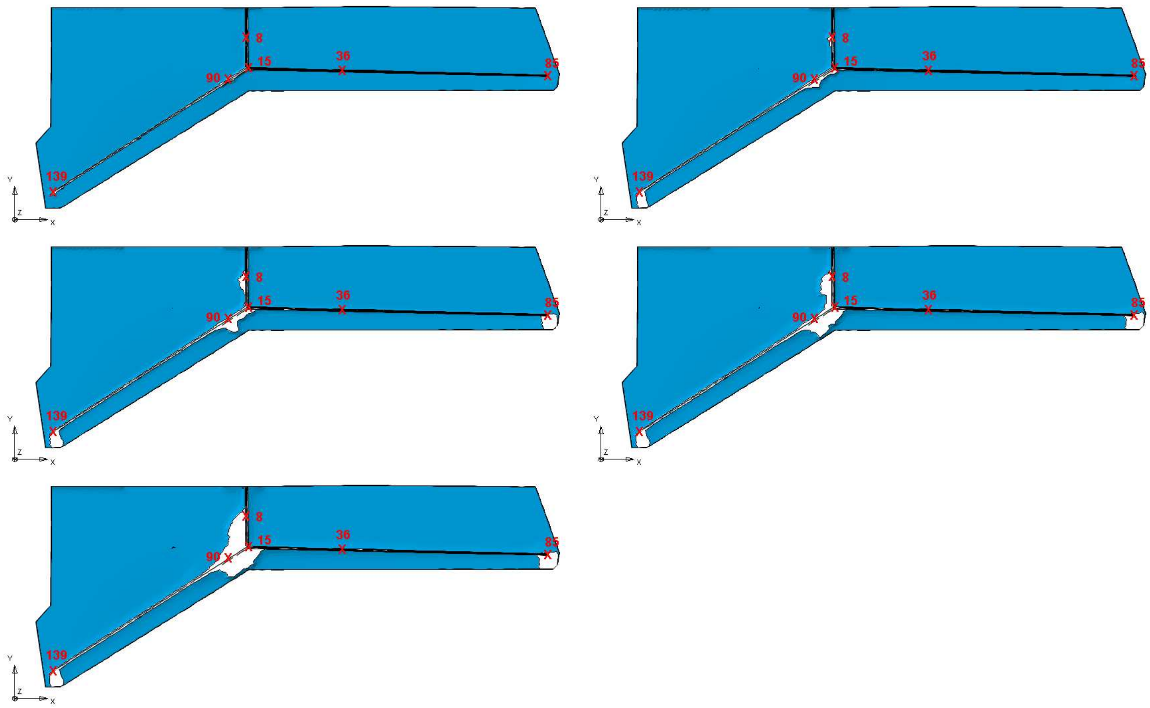

Figure 8. Water table of 3D subsurface flow at various times: Time = 3 hours at Top Left, Time = 6 hours at Top Right, Time = 12 hours at Middle Left, Time = 24 hours at Middle Right, Time = 36 hours at Bottom; The area of no-shade has water table above ground surface.

the underlying 3D subsurface grid, large 2D elements may also imply large aspect ratios on 3D elements, which would cause inaccurate 3D results or linear/nonlinear convergence problems when the unsaturated zone exists. On the other hand, for a large watershed with shallow aquifers underneath, an appropriate aspect ratio may be represented by fairly small horizontal meshes and make the computation unachievable as a consequence. One possible solution for this dilemma may be the use of large horizontal meshes for surface flow computation and small horizontal meshes that would maintain acceptable aspect ratios for 3D subsurface computation.

5. SUMMARY

This paper, through a hypothetic example, demonstrates the capability of the WASH123D model in studying a spreader swale system for the modeling of surface and subsurface hydrologic interactions in a South Florida watershed near the Biscayne Bay. It is thus encouraging that WASH123D can be used to help design a spreader swale system, where many factors, such as the flow rate of inflow, the length and dimension of spreader swale, the roughness of canal/overland surface, subsurface saturation index, subsurface material, rainfall, and boundary conditions may play crucial roles. In the future, efforts to address the issues aforementioned in the Discussion section should be invested.

REFERENCES

1. U. S. Government, State of Florida, , and Others. Comprehensive Everglades Restoration Plan (CERP). http://www.evergladesplan.org/.
2. G. T. Yeh, H. P. Cheng, F Zhang G. Huang, H. C. Lin, E. Edris, , and D. Richards. A numerical model of flow, heat transfer, and salinity, sediment, and water quality transport in watershed systems of 1d stream-river network, 2d overland regime, and 3d subsurface media (WASH123D: Version 2.0). Technical Report CHL-03-XX, Engineer Research and Development Center, U.S. Army Corps of Engineers, MS 39180-6199, November 2003.
3. G. T. Yeh, G. Huang, and H. C. Lin. A first principle, physics-based watershed model of various temporal and spatial scales, world water and environmental resources congress, speciality symposium of integrated surface and groundwater modeling. In *ASCE 2003 CD-ROM*, Philadelphia, Pennsylvania, USA, June 22-26, 2003.
4. H. C. Lin, D. R. Richards, G. T. Yeh, J. R. Cheng, H. P. Cheng, and N. L. Jones. FEMWATER: A three-dimensional finite element computer model for simulating density-dependent flow and transport in variably saturated media. Technical Report CHL-97-12, Engineer Research and Development Center, U.S. Army Corps of Engineers, MS 39180-6199, July 1997.